A Second Luminous Blue Variable in the Quintuplet Cluster

T. R. Geballe

Gemini Observatory, 670 N. A'ohoku Pl., Hilo, HI 96720

F. Najarro

Instituto de Estructura de la Materia, CSIC, Serrano 121, 28006 Madrid, Spain

and

D. F. Figer

Space Telescope Science Institute, 3700 San Martin Drive, Baltimore, MD 21218

Received ______________________; accepted ______________________

to be published in The Astrophysical Journal Letters

ABSTRACT

H and K band moderate resolution and 4 μm high resolution spectra have been obtained for FMM#362, a bright star in the Quintuplet Cluster near the Galactic Center. The spectral features in these bands closely match those of the Pistol Star, a luminous blue variable and one of the most luminous stars known. The new spectra and previously-obtained photometry imply a very high luminosity for FMM#362, $L \geq 10^6 L_\odot$, and a temperature of 10,000 – 13,000 K. Based on its luminosity, temperature, photometric variability, and similarities to the Pistol Star, we conclude that FMM#362 is a luminous blue variable.

Subject headings: stars: evolution — stars: mass-loss — stars: variables: other — Galaxy: center — ISM: individual (G0.15-0.05)

1. Introduction

The Quintuplet Cluster (AFGL 2004), roughly 30 pc in projection from the nucleus of the Galaxy, contains a number of massive and luminous stars which are not detected at visible wavelengths due to heavy extinction by dust along the line of sight. Some of the brightest of these stars are enshrouded by circumstellar dust and have featureless infrared spectra, apart from interstellar absorption bands (Okuda et al. 1990). Others are not enshrouded and show line absorption and emission from their photospheres and winds. Cotera et al. (1996) and Figer et al. (1998, hereafter F98) have demonstrated that one such object, originally reported as object No. 25 by Nagata et al. (1993), first singled out by Moneti, Glass & Moorwood (1994), and now known as the Pistol Star, has a luminosity of $\sim 10^7$ $L_\odot$, making it one of the most luminous stars known. Figer, McLean and Morris (1995) suggested that this star is a luminous blue variable (LBV), a hypothesis supported by its position in the HR diagram (F98), photometric variability (Glass et al 1999; Figer, McLean, & Morris 1999a, hereafter FMM99), and circumstellar ejecta (Figer et al. 1999b).

FMM99 have recently identified a second candidate LBV in the Quintuplet Cluster, their source 362, hereafter FMM#362. The identification was based on the star's infrared brightness, photometric variability (confirmed by Glass et al. 1999), and a low-resolution spectrum obtained by Figer (1997, unpublished). Photometry by FMM99 and by Glass et al. suggest that at maximum FMM#362 is nearly as bright as the Pistol Star.

2. Observations and Data Reduction

We have obtained spectra of FMM#362 in the H and K bands and near 4 μm at UKIRT with the facility 1-5 μm grating spectrometer, CGS4, which was configured with a 256x256 InSb array and a 0.6” (one-pixel) wide slit. An observing log is provided in Table 1.

The nearby featureless Quintuplet source GCS 3-2 (Nagata et al 1990, Okuda et al. 1990; also listed as source 2 by Glass et al 1990; as source 24 in Nagata et al 1993 and source VR 5-2 in Moneti, Glass & Moorwood 1994) was used as a comparison star, although it is a suspected variable (Glass et al. 1999).

The H and K spectra were wavelength-calibrated with the aid of arc lamp spectra. The 4 μm spectrum was wavelength-calibrated by comparison to the spectrum of the planetary nebula NGC 6572 (V_{hel} = −9 km s^{-1}). Flux calibration in the H and K bands assumed that the dereddened spectrum of GCS 3-2 is that of a 889 K blackbody (Okuda et al. 1990) with K = 6.28 (Glass et al. 1999). Because of the uncertainty in this approximation, the line fluxes far from 2.2 μm and the overall spectral shape are probably not accurate. From our data we derive K=7.5 for FMM#362. The brightness is consistent with previous photometry. We believe that our relative spectrophotometry is accurate to ±20%.

3. Results and Initial Analysis

The low resolution K-band spectrum of FMM#362 from 1999 is shown in Fig. 1 and the higher resolution spectra are shown in Figs. 2 – 4. Measured parameters of detected lines are given in Table 2. We note a modest, but significant weakening of those spectral lines (2.10–2.18 μm) observed on both dates. In spectral intervals where both the Pistol Star and FMM#362 have been measured, their spectra are quite similar. In addition to lines of hydrogen, the same permitted lines of sodium, magnesium, and iron are in emission in both stars and the He I lines, where clearly detected, are in absorption. The principal difference between the spectra is the lower equivalent widths of lines (in particular those of hydrogen) in FMM#362. A possible additional difference between the two stars is that forbidden lines are clearly seen only in the Pistol Star. However, these are weak and, considering the smaller equivalent widths of the lines in FMM#362, non-detections there are probably not surprising.

The 4 μm spectrum (Fig. 2) is dominated by a strong hydrogen Br α line at 4.05 μm, which because of its strength and equivalent width appears more suitable than other lines for providing accurate velocity information. The He I 5-4 triplet line, shifted -240 km s^{-1} relative to Br α, is weak but clearly present. Although the core of the Br α line is symmetric, even after allowing for the He I line there is considerably more emission at high negative velocities than at high positive velocities. This is caused by continuum opacity (Najarro et al 1998a), which weakens the redshifted emission wing, an effect also evident in the Pistol Star (Figer et al. 1998). We estimate that in FMM#362 the wings extend roughly to -250 km s^{-1} and +125 km s^{-1} from the peak, somewhat further than those of the Pistol Star. The velocity of peak emission is $+121 \pm 15$ km s^{-1} (LSR). This is very close to the velocity of 130 km s^{-1} determined for the Pistol Star (F98) and other members of the cluster (Figer 1995), clearly establishing FMM#362 as a cluster member.

A number of Si II, Mg II and Fe II lines are prominent in Figs. 3-4. The Si II $5s^2S_{1/2}$-$5p^2P_{3/2}$ 1.691 μm and $5s^2S_{1/2}$-$5p^2P_{1/2}$ 1.698 μm doublet is a powerful diagnostic tool, as it appears in emission for only a very narrow range of stellar temperatures and wind density structures, indicating the presence of amplified NLTE effects (Najarro et al., in preparation). Several of the Mg II lines observed in the H and K-bands have the $5p^2P$ level in common. Those with it as the upper level (the 2.13/14 μm and 2.40/41 μm doublets) are much stronger than those with it as a lower level (in the H band), revealing that pumping through the resonance $3s^2S$-np^2P lines must be a significant populator of the np^2P levels. Two types of lines are found for Fe II: the so-called semi-forbidden lines (denoted in Table 2 and in the figures by single left-hand brackets) such as Fe II $z^4F_{9/2}$-$c^4F_{9/2}$ 1.688 μm and Fe II $z^4F_{3/2}$-$c^4F_{3/2}$ 2.089 μm with very weak oscillator strengths (gf$\sim$$10^{-5}$) which form in the outer stellar wind; and permitted (gf$\sim$1) lines connecting higher lying levels, such as the e^6G-$5p^6F$ lines near 1.733 μm, which form much closer to the atmosphere.

Except for Br α (5–4), the rest of the observed Brackett series lines (11–4, 10–4, and 7–4) show P Cygni profiles with the emission strengthening and absorption weakening with decreasing series number. This is expected in a dense wind where line emission increasingly overwhelms the absorption profiles for lower series (higher oscillator strength) lines, since these form further away from the photosphere. The same trend is seen in the Humphreys series (14–6) hydrogen line at 4.02 μm. Because of non-negligible continuum opacity effects at 4 μm, Br α can only provide a lower limit to V_∞. The Fe II $z^4F_{9/2}$-$c^4F_{9/2}$ 1.688 μm line profile is much less influenced by opacity effects. From it we estimate V_∞ to be ≈160 km s^{-1}.

Finally, it is noteworthy that the 1.700 μm and 2.112 μm lines of He I appear weakly in absorption, while the He I 2.06 μm line is not convincingly detected and the He I(5–4) emission components around Br α are very weak. This behavior, together with the complete absence of He II lines, is a strong indicator of a low temperature (and low ionization state).

4. Discussion

4.1. FMM#362 as an LBV

A rough estimate of basic stellar parameters of FMM#362 can be made by comparison of its spectrum with that of the Pistol Star, for which values have been derived (F98). In particular, the presence of the He I lines in absorption as well as observed ratio of the Fe II 2.089 μm and Mg II 2.14 μm lines tightly constrain the parameters of FMM#362 as they did for the Pistol Star. For the Pistol Star two families of models with T_{eff} = 14,000 K, L = $10^{6.6}L_\odot$ and T_{eff} = 21,000 K, L = $10^{7.2}$ $L_\odot$ fit the R ≈ 1,000 infrared spectra. New higher resolution spectra of the Pistol Star (Najarro et al. 1998b), when analyzed with the model atmospheres of Hillier and Miller (1998), favor the lower temperature solution. Given the similarities in their spectra, the effective temperature of FMM#362 probably also is low; additional support for this is given in section 4.3. Monitoring has shown that the stars are nearly the same average brightness at K, whereas in 1996 the Pistol Star was 0.5 mag brighter than FMM#362 at J band (Figer, McLean and Morris 1996). Assuming that the two stars have the same temperature and that in FMM#362 the infrared bound-free and free-free excess in the continuum is negligible (as is the case for the Pistol Star below 3 μm), their luminosity ratio is given by the extinction-corrected flux ratio. From the close proximity of the two stars it is reasonable to assume that the extinctions are the same, indicating that FMM#362 is at least half as luminous as the Pistol Star.

4.2. Two LBVs in the Quintuplet Cluster?

As there are only about a half dozen LBVs known in the Galaxy (Nota et al. 1995), one must question the identification of two LBVs in a single cluster. However, the Quintuplet is one of the most massive young clusters in the Galaxy, containing over 150 O-stars at birth (FMM99) and LBVs are thought to be evolved O-stars (see Langer et al. 1994 for one proposed evolutionary sequence). The cluster age, 4 Myr (FMM99), is that when O-stars should be evolving through the LBV stage. The number of cluster LBV stars at any time during this stage is roughly $N_{LBV} = (\tau_{LBV}\mathrm{lifetime})/(\tau_{LBV-p}/N_{O-stars}) = 25{,}000$ yr/(6 Myr/150 O-stars) = 2/3, where τ_{LBV-p} is the production timescale. There are many uncertainties in this estimate: e.g., the assumptions that all O-stars become LBVs; that the LBV lifetime is roughly equal to the ratio of known galactic LBVs to known galactic O-stars times a typical O-star lifetime; and that the O-stars become LBVs at a constant rate. Nevertheless, we conclude that it is not unreasonable to find two LBVs in this cluster.

4.3. Qualitative analysis

The equivalent widths of the emission lines in FMM#362 are lower than in the Pistol Star, not only for hydrogen, but also for Si II, Mg II, Na I, and Fe II. This suggests that the stellar wind of FMM#362 is less dense than that of the Pistol Star. Our inference that the bound-free and free-free contributions to the continuum are insignificant below 3 μm lead us to conclude that the equivalent widths of the emission lines are proportional to the wind density (see Simon et al 1983 or Najarro 1995) and hence that the value of $\dot{\mathrm{M}}V_\infty/\mathrm{R}^2$ for FMM#362 is roughly a factor of two less than for the Pistol Star. From luminosity considerations we estimate $(\mathrm{R}^*_{Pistol}/\mathrm{R}^*_{362})^2 \approx 1.5$. Taking into account the scaling equations for $\dot{\mathrm{M}}$ and R (Najarro et al 1997) and that $V_{\infty 362} \approx 160$ km s^{-1} (from the Fe II 1.688 μm line) we conclude that $\dot{\mathrm{M}}_{Pistol} \approx 1.5\ \dot{\mathrm{M}}_{362}$.

Important constraints on the stellar temperature (ionization) are set by the weakness of the He I 2.06 μm line and especially by the weakness of the He I (5-4) components near 4.05 μm. The observed ratio of the H and He I component exceeds by a large factor the expected value even for cosmic He I value, if there were any significant amount of He II in the wind. This indicates that He II must recombine to He I very close to the photosphere, implying an upper limit of around 13,000 K for the temperature of the object. A lower limit on the effective temperature is set by the non-detection of the $3s^23p^2S_{1/2}$-$3s^24p^2P_{3/2}$ 2.180 μm and $3s^23p^2S_{1/2}$-$3s^24p^2P_{1/2}$ 2.209 μm intercombination lines of Si II in absorption (note that the latter would be contaminated by Na I emission), since these lines are expected to be in absorption if the temperature is below 10,000 K.

From the observed weak He I lines one might easily conclude that helium is not enhanced at all. However, preliminary analysis (Najarro et al, in preparation) shows that an enhancement as large as He/H$\sim$1 can be completely masked. Only the 2.06 μm line is strengthened by increasing He/H to this value, but the strength of this line also depends strongly on blanketing. The spectrum of FMM#362 at 2.06 μm has been observed at low resolution only. Therefore, although we suspect that the value of He/H is not far from normal, we cannot rule out a much higher value.

Finally, we consider the abundances of Mg, Si, and Fe. The striking similarity of the Mg II lines in FMM#362 to those in the Pistol Star support a higher than solar Mg abundance for FMM#362 (Najarro et al 1998b). The case of the Si II lines is different. Although in principle a high Si abundance is needed to obtain the H band lines in emission, the behavior of these lines is controlled to first order by the wind density structure and to second order by the effective temperature. Different velocity fields and transition zones between photosphere and wind can easily mask a factor of five change in Si abundance (producing similar Si II 1.7 μm emission line strengths and profiles), even if the stars have the same effective temperature, radius, and mass-loss rate.

To derive the iron abundance two sets of Fe II lines can be used. The z^4F-c^4F lines are formed in the outer regions of the wind where the levels suffer from severe departures from LTE. Line strengths are extremely sensitive to the ionization structure of Fe in the outer wind. Initial tests (Najarro et al 1998b) showed that a high iron abundance is required to reproduce these semi-forbidden lines. However, if charge exchange reactions $Fe^{++} + H \longleftrightarrow Fe^{+} + H^{+}$ are included (see Oliva et al 1989 and Hillier 1998), the ionization structure of Fe can be dramatically altered in the outer parts of the wind, producing a net enhancement of Fe II and increased strengths of the semi-forbidden lines, implying a lower Fe abundance. The e^6F-$5p^6D$ transitions, arising from higher lying levels which are formed much closer to the star's photosphere, also are available. Their successful use as abundance diagnostics depends crucially on the reliability of the atomic Fe II data. For the important infrared lines of Fe II important discrepancies exist between the best two available datasets: the Iron Project data (Seaton et al. 1994) and the data of Kurucz (1999). First tests using an model Fe II atom which optimizes both datasets for the e^6F-$5p^6D$ transitions favor an Fe abundance not very far from solar, a value that has been recently found by Carr et al (1999) for the Galactic Center source IRS 7. Thus both Fe II line diagnostic methods may converge to a unique iron abundance and the derived iron abundance may be compatible with the enhanced magnesium and silicon values.

It is necessary to perform accurate quantitative analysis to obtain more realistic estimates of the metallicity and stellar parameters of FMM#362. We have begun such work following the method described in Najarro et al (1998b); the results will be presented in detail elsewhere (Najarro et al, in preparation).

The United Kingdom Infrared Telescope is operated by the Joint Astronomy Centre on behalf of the U.K. Particle Physics and Research Council. We thank the staff of the Joint Astronomy Centre for its support of these measurements. We also are grateful to D. J. Hillier for his atmospheric code. F. Najarro acknowledges grants of the DGYCIT under PB96-0883 and ESP98-1351.

Table 1. Observing Log for FMM#362.

UT Date	range (μm)	resolution (μm)	sampling (res. el.)	Integ. (sec.)
19980802	1.90-2.54	0.0025	1/3	480
19980802	1.40-2.04	0.0025	1/3	480
19990422	1.87-2.51	0.0025	1/3	240
19990422	3.94-4.10	0.00065	1/2	640
19990504	2.10-2.18	0.00033	1/3	720
19990504	1.67-1.75	0.00033	1/3	480

Table 2. Detected Spectral Lines in FMM#362

Ion	Transition $l - u$	λ(Lab) vac. μm	λ(Obs) vac. μm	W_λ 10^{-4} μm
1999 April 22:				
He I	$3p^1P$-$4d^1D$	1.909	1.910	-0.6
H I	4 – 8	1.945	1.945	1.4
[Fe II	$z^4F_{5/2}$-$c^4F_{5/2}$	1.975	1.975	1.9
[Fe II]	$a^2G_{9/2}$-$a^2H_{9/2}$	2.016	2.016	0.9
[Fe II	$z^4F_{3/2}$-$c^4F_{3/2}$	2.089	2.089	2.4
He I	$3p^3P$-$4s^3S$ + $3p^1P$-$4s^1S$	2.113	2.112	-2.2
Mg II	$5s^2S_{1/2}$-$5p^2P_{3/2}$	2.137	2.137	2.4
Mg II	$5s^2S_{1/2}$-$5p^2P_{1/2}$	2.144	2.144	1.7
H I	4 – 7	2.166	2.166	5.2
Si II	$6p^2P_{3/2}$-$6d^2D_{5/2,3/2}$	2.200 bl	2.201	0.3
Na I	$4s^2S_{1/2}$-$4p^2P_{3/2,1/2}$	2.208 bl	2.208	0.6
[Fe II	$z^4D_{3/2}$-$c^4P_{3/2}$	2.241	2.241	0.5
H I	5 – 27	2.360	2.361	0.6
H I + Fe II	5 – 26 + $e^4F_{7/2}$-$5p^4D_{5/2}$	2.367+2.368	2.368	0.9
H I	5 – 25	2.374	2.374	0.5
H I	5 – 24	2.383	2.383	0.6
H I	5 – 23	2.392	2.392	0.9
H I + Mg II	5 – 22 + $4d^2D_{5/2}$-$5p^2P_{3/2}$	2.404+2.405	2.404 br	3.1
Mg II + H I	$4d^2D_{3/2}$-$5p^2P_{1/2}$ + 5-21	2.413+2.416	2.414 br	2.5
H I	5 – 20	2.431	2.431	1.2
H I	5 – 19	2.449	2.449	1.0
H I	6 – 14	4.021	4.022	2.6
He I	$4f^{1,3}F$-$5g^{1,3}G$	4.049	4.050	5.0
H I	4 – 5	4.052	4.053	68.

Table 2—Continued

Ion	Transition l – u	λ(Lab) vac. μm	λ(Obs) vac. μm	W_λ 10^{-4} μm
1999 May 4:				
Mg II	$5p^2P_{1/2}$-$5d^2D_{3/2}$	1.676	1.676	0.62
[Fe II	$z^4F_{9/2}$-$c^4F_{7/2}$	1.679	1.679	0.33
Mg II	$5p^2P_{3/2}$-$5d^2D_{5/2}$	1.680	1.680	0.28
H I	4 – 11	1.681	1.681	-0.58
[Fe II	$z^4F_{9/2}$-$c^4F_{9/2}$	1.688	1.688	4.0
Si II	$5s^2S_{1/2}$-$5p^2P_{3/2}$	1.691	1.691	1.5
Si II	$5s^2S_{1/2}$-$5p^2P_{1/2}$	1.698	1.698	0.98
He I	$3p^3P$-$4d^3D$	1.701	1.701	-0.98
Fe II	$e^6F_{11/2}$-$5p^6D_{9/2}$	1.704	1.704	0.12
Si II	$5f^2F$-$6g^2G$	1.719	1.719	0.23
Fe II	$e^6G_{9/2}$-$5p^6F_{7/2}$	1.732	1.732	0.12
Fe II	$e^6G_{11/2}$-$5p^6F_{9/2}$	1.733	1.733	0.24
H I + He I	4 – 10	1.737	1.737	-1.2
Fe II	$e^6F_{9/2}$-$5p^6D_{9/2}$	1.741	1.741	0.60
Mg II	$5p^2P_{1/2}$-$6s^2S_{1/2}$	1.742	1.742	1.0
Mg II	$5p^2P_{1/2}$-$6s^2S_{1/2}$	1.746	1.746	1.0
HeI	$3p^3P$-$4s^3S$	2.113	2.113	-0.79
HeI	$3p^1P$-$4s^1S$	2.114	2.114	-0.42
MgII	$5s^2S_{1/2}$-$5p^2P_{3/2}$	2.137	2.138	1.9
MgII	$5s^2S_{1/2}$-$5p^2P_{1/2}$	2.144	2.145	1.0
FeII	$6s^6D_{9/2}$-$6p^6D_{9/2}$	2.145	2.146	0.24
HeI	$4f^3F$-$7z^3Z$	2.165	2.166	-0.19
H+HeI	4 – 7	2.166	2.167	4.0

REFERENCES

Carr, J. S., Sellgren, K. & Balachandran, S. C. 1999, ApJ, in press

Cotera, A. S., Erickson, E. F., Colgan, S. W. J., Simpson, J. P., Allen, D. A. & Burton, M. G. 1996, ApJ, 461, 750

Figer, D. F. 1995, Thesis, UCLA

Figer, D. F., McLean, I. S. & Morris, M. 1996, in "The Galactic Center", R. Gredel, ed., ASP Conf Series, 102, 263

Figer, D. F., McLean, I. S. & Morris, M. 1999a ApJ, 514, 202 (FMM99)

Figer, D. F., Morris, M., Geballe, T. R., Rich, R. M., McLean, I. S., Serabyn, E., Puetter, R., & Yahil, A. 1999b, ApJ, 525, 759

Figer, D. F., Najarro, F., Morris, M., McLean, I. S., Geballe, T. R., Ghez, A. M. & Langer, N. 1998, ApJ, 506, 384 (F98)

Glass, I. S., Moneti, A. & Moorwood, A. F. M. 1990 MNRAS, 242, 55P

Glass, I. S., Matsumoto, S., Carter, B. S. & Sekiguchi, K. 1999, MNRAS, 304, L10

Hillier, D. J. 1998, in "Proceedings of IAU Symposium No. 189 T. R. Bedding, A. J. Booth & J. Davis, eds., Kluwer (Dordrecht), 209

Hillier, D. J. & Miller, D. L. 1998, ApJ, 496, 407

Langer, N., Hamann, W.-R., Lennon, M., Najarro, F., Pauldrach, A. W. A. & Puls, J. 1994, A&A, 290, 819

Kurucz, R., L., 1999 Kurucz CD-ROM 24, (Cambridge: Smithsonian Astrophysical Observatory; see http://cfaku5.harvard.edu/)

Moneti, A., Glass, I. S. & Moorwood, A. F., M. 1994, MNRAS, 268, 194

Nagata, T., Hyland, A. R., Straw, S. M., Sato, S. & Kawara, K. 1993, ApJ, 406, 501 1193

Nagata, T., Woodward, C. E., Shure, M., Pipher, J. L. & Okuda, H. 1990, ApJ, 351, 83

Najarro, F. 1995, Thesis

Najarro, F., Hillier, D. J. & Stahl, O., 1997, A&A, 326, 1117

Najarro, F., Kudritzki, R. P., Hillier, D. J., Lamers, H. J. G. L. M., Voors, R. H. M., Morris, P. W. & Waters, L. B. F. M., 1998a in "Boulder-Munich Workshop II: Properties of hot luminous stars", Ed. I. D. Howarth, ASP Conf. Series, Vol 131, 57

Najarro, F., Hillier, D. J., Figer, D. F. & Geballe, T. R. 1998b, in "The Central Parsecs, Galactic Center Workshop 1998", eds. H. Falcke, A. Cotera, W. Huschl, F. Melia, and M. Rieke, in press.

Nota, A., Livio, M., Clampin, M., Schulte-Ladbeck, R. 1995, ApJ, 448, 778

Okuda, H., Shibai, H., Nakagawa, T., Matsuhara, H., Kobayashi, Y., Kaifu, N., Nagata, T., Gatley, I. & Geballe, T. R. 1990, ApJ, 351, 89

Oliva, E.; Moorwood, A. F. M. & Danziger, I. J. 1989, A&A, 214, 307

Seaton, M. J., Yan Y., Mihalas, D. & Pradhan, A. K. 1994, MNRAS, 266, 805

Simon, M. Felli, M. Massi, M., Cassar, L. & Fischer, J. 1983, ApJ, 266, 623

Fig. 1.— K-band Spectrum of FMM#362, flux-calibrated using the spectrum of the featureless Quintuplet object GCS3-2 (assumed to be a blackbody of temperature 889 K), in the H and K bands, obtained on 1999 April 22. No dereddening was applied. The slightly smoothed spectrum has a resolution of $\sim$0.0030 μm (400 km s^{-1}). Strong lines are labelled; see Table 2 for a complete listing of detected lines.

Fig. 2.— Unsmoothed spectrum of FMM#362 at 4 μm, obtained on 1999 April 22, divided by that GCS3-2. The resolution is 0.00065 μm (50 km s^{-1}).

Fig. 3.— Slightly smoothed spectrum (1.67-1.75 μm) of FMM#362, obtained on 1999 May 4; the resolution is 0.00040 μm ($\sim$70 km s^{-1}).

Fig. 4.— Slightly smoothed spectrum (2.10-2.18 μm) of FMM#362, obtained on 1999 May 4; the resolution is 0.00040 μm ($\sim$55 km s^{-1}).

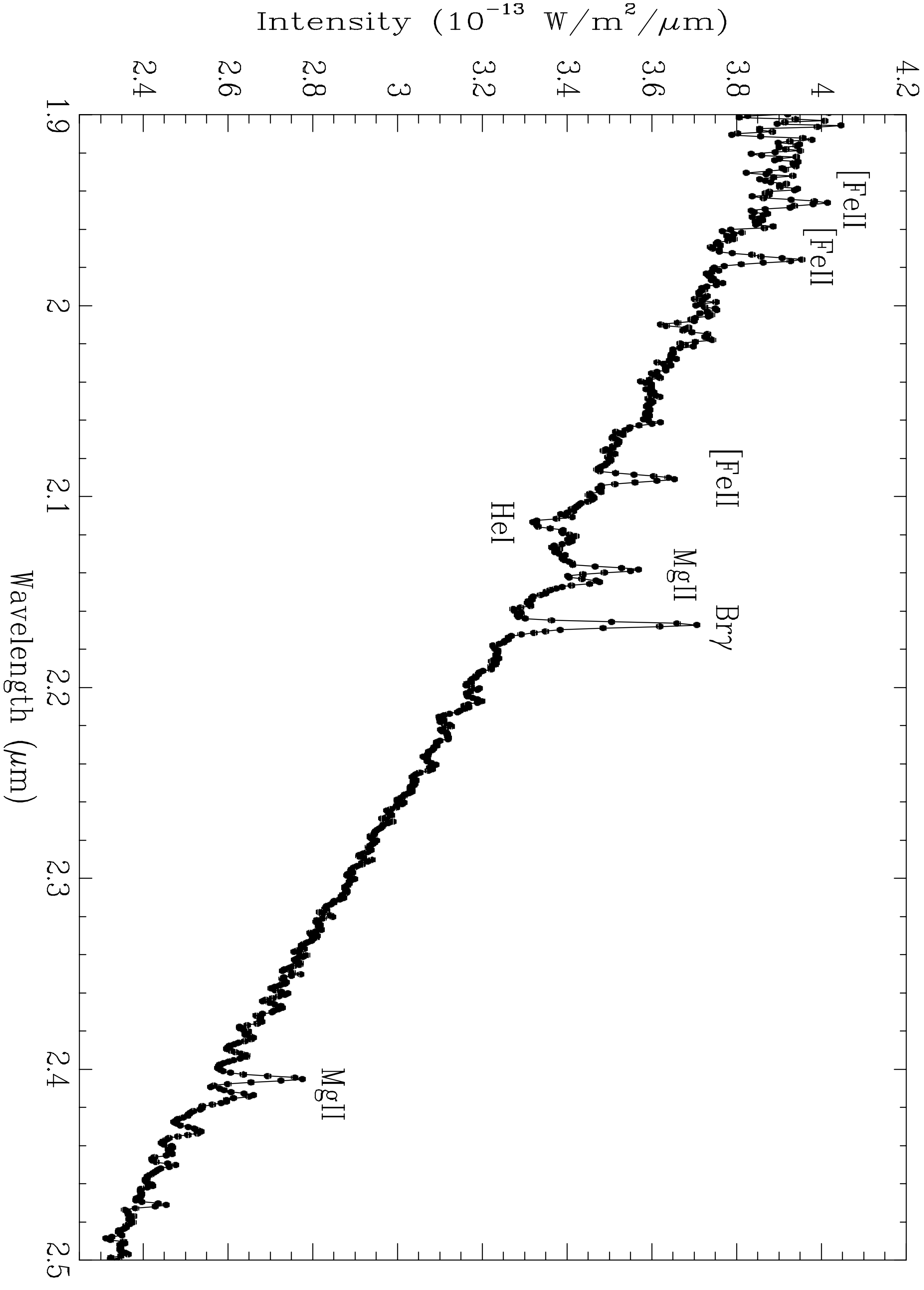
Intensity (10^{-13} W/m^2/μm)
Wavelength (μm)
[FeII
[FeII
[FeII
HeI
MgII
Brγ
MgII
2.4
2.6
2.8
3
3.2
3.4
3.6
3.8
4
4.2
1.9
2
2.1
2.2
2.3
2.4
2.5

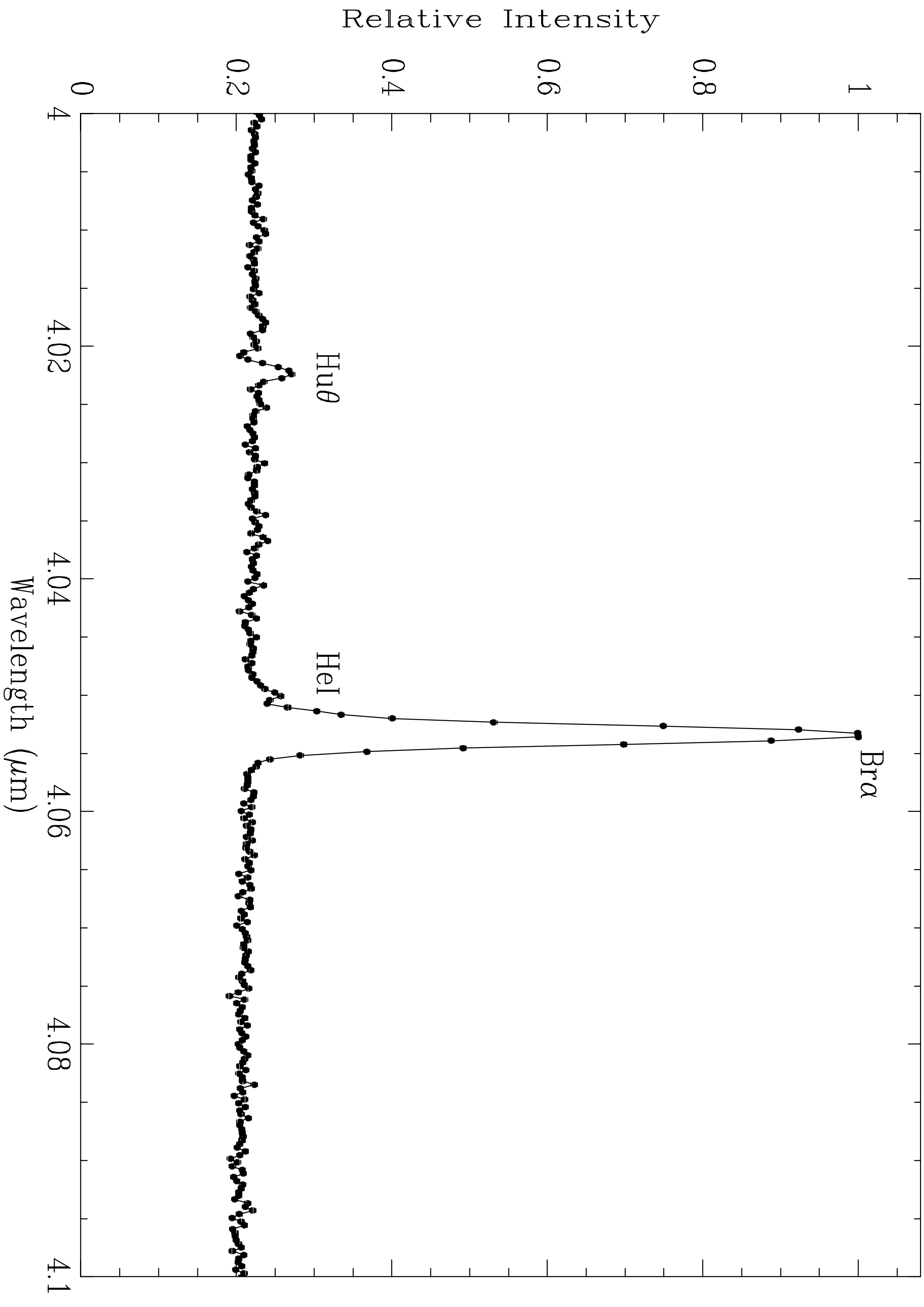

Relative Intensity
0
0.2
0.4
0.6
0.8
1
4
4.02
4.04
4.06
4.08
4.1
Wavelength (μm)
Huθ
HeI
Brα

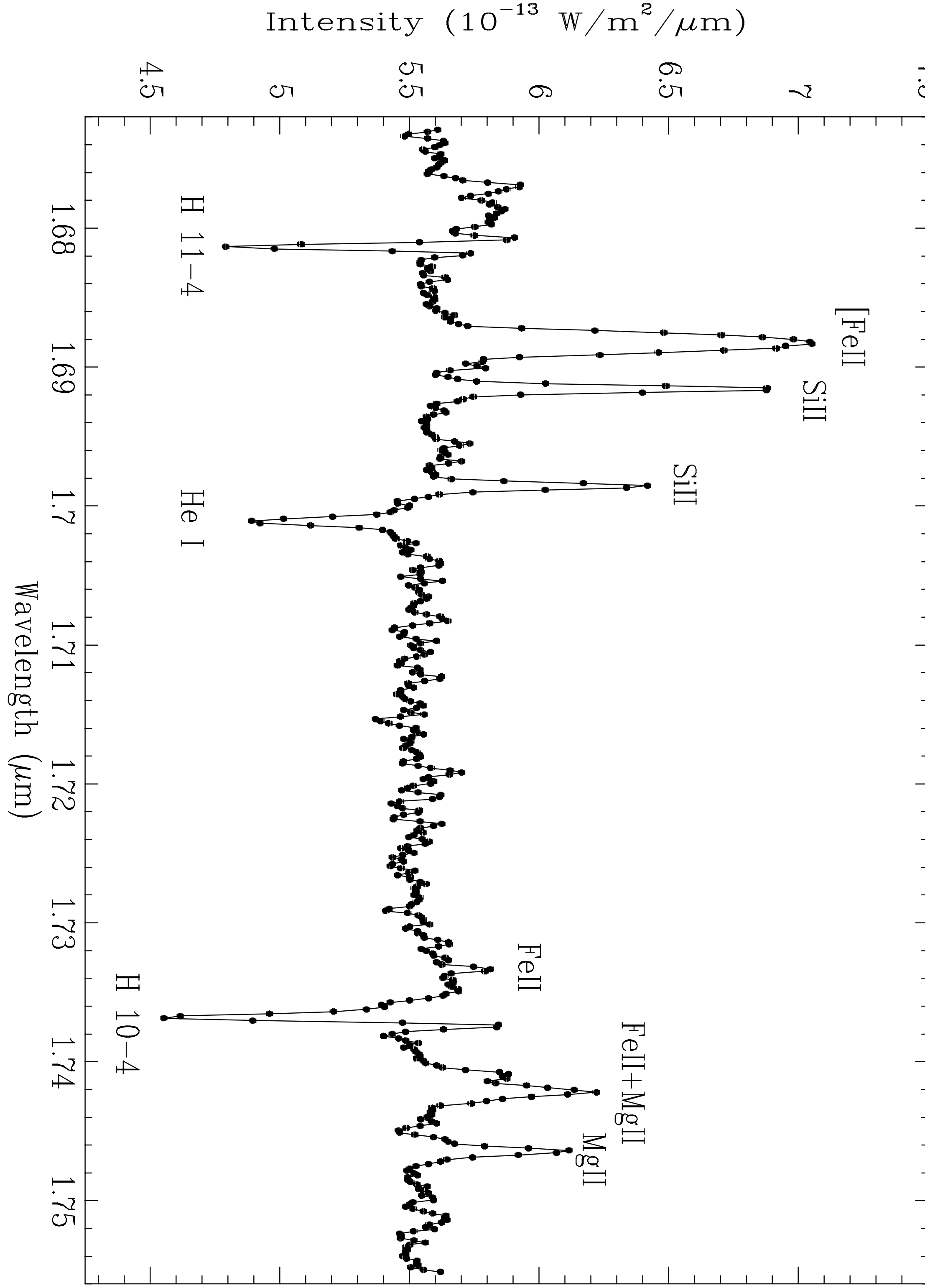

Intensity (10^{-13} W/m^2/μm)
Wavelength (μm)
H 11–4
[FeII
SiII
SiII
He I
FeII
H 10–4
FeII+MgII
MgII

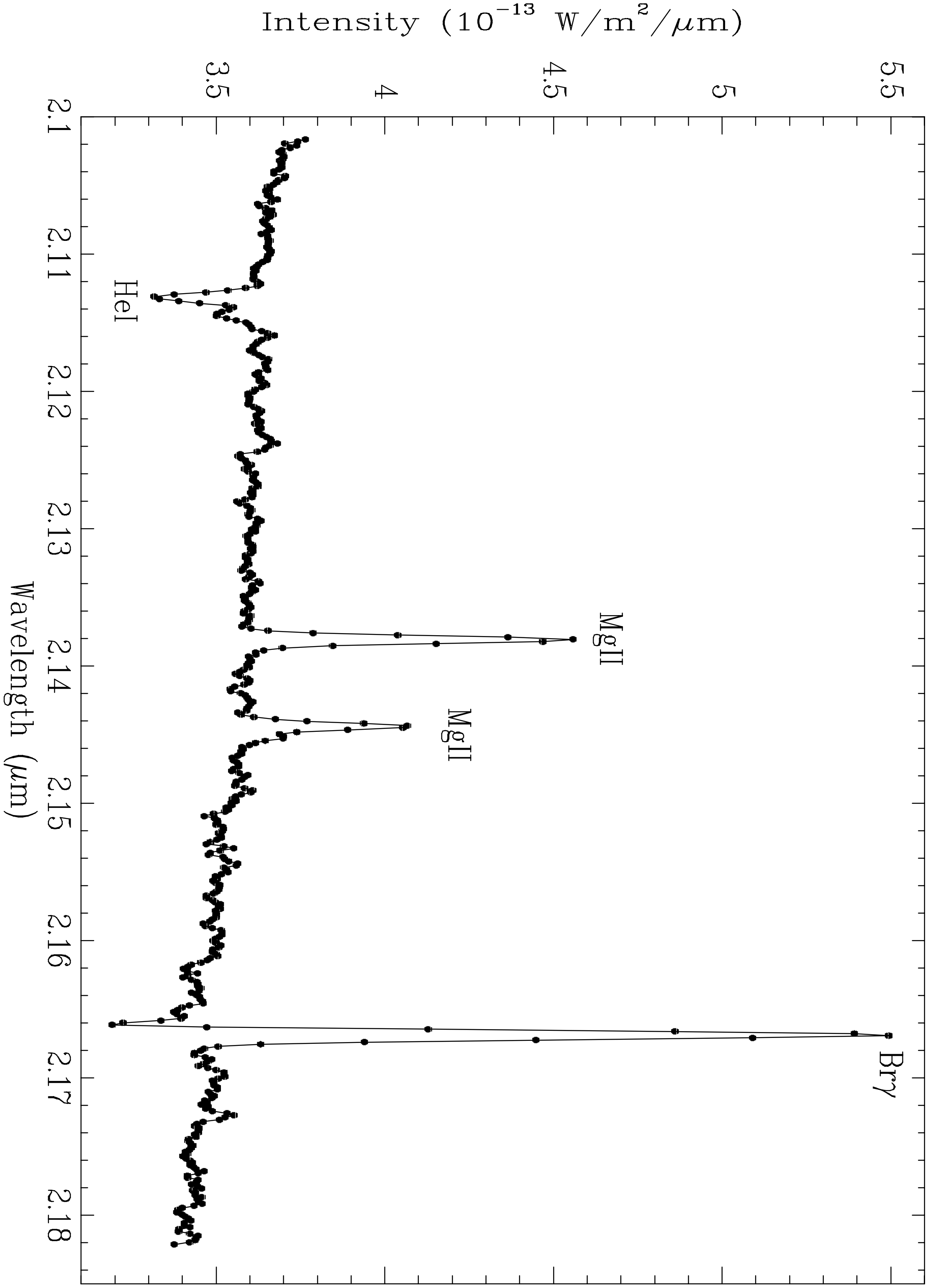

Intensity (10^{-13} W/m^2/μm)
3.5
4
4.5
5
5.5
2.1
2.11
2.12
2.13
2.14
2.15
2.16
2.17
2.18
Wavelength (μm)
HeI
MgII
MgII
Brγ